

# Experimental Evaluation of Hydraulic Jump Characteristics in Gradually Expanding Sloping Channel

S. K. Gupta<sup>†</sup> and V. K. Dwivedi

*Department of Mechanical Engineering, IET, GLA University Mathura, UP, 281406, India*

<sup>†</sup>Corresponding Author Email: [sanjeev.gupta@gla.ac.in](mailto:sanjeev.gupta@gla.ac.in)

## ABSTRACT

Understanding hydraulic jumps in gradually expanding sloping channels is crucial for designing eco-friendly water management systems that minimize environmental impacts. This study seeks to investigate how the expansion ratio and channel slope together influence the characteristics of hydraulic jumps. The experiments were performed on four different channel slopes ( $0^\circ$ ,  $2^\circ$ ,  $4^\circ$ , and  $6^\circ$ ) and four distinct expansion ratios ( $B = b_1/b_2$ ) of 0.35, 0.45, 0.55 and 0.75. The Reynolds number was ranged from 7150 to 27750, while the Froude number varied between 2.5 and 8.5 during the experiments. Novel correlations were developed to predict key hydraulic jump parameters, including depth ratio ( $d_2/d_1$ ), relative energy loss ( $E_L/E_1$ ) and relative jump length ( $L_j/d_1$ ), by considering the effects of expansion ratio, channel slope and Froude number. The results indicate that as the channel slope increased from  $0^\circ$  to  $6^\circ$ , the depth ratio and relative energy loss increased by approximately 30.53% and 15.37%, respectively, while the relative jump length decreased by 11.11%. Conversely, as the expansion ratio decreased from 1.0 to 0.35, the depth ratio and relative jump length were reduced by approximately 9.63% and 10.42%, respectively; while the relative energy loss was increased by 24.21%. These findings highlight the significant influence of channel geometry on hydraulic jump characteristics, offering valuable insights for optimizing water conveyance structures. The proposed correlations provide a novel and intuitive approach to analyze hydraulic jumps in expanding sloping channels, addressing gaps in existing literature and contributing to sustainable water resource management.

## Article History

Received October 28, 2024  
Revised February 7, 2025  
Accepted February 16, 2025  
Available online May 5, 2025

## Keywords:

Froude number  
Energy dissipation  
Reynolds number  
Depth ratio  
Empirical correlation

## 1. INTRODUCTION

A hydraulic jump occurs when a rapidly flowing fluid, such as water, suddenly slows down and transitions into a slower, turbulent flow. This transition creates a distinct and visible rise in the water's surface (Gupta et al., 2013; Hafnaoui & Debabeche, 2023; Hasanabadi et al., 2023). Hydraulic jumps are often necessary in sloping expanding channels due to several reasons: (i) Energy Dissipation: In a sloping channel, the water flow gains kinetic energy as it moves downhill. If the flow were to continue without any energy dissipation, it could lead to excessive erosion and instability downstream. A hydraulic jump acts as a natural energy dissipater, converting the excess kinetic energy into turbulence and heat, reducing the flow velocity and preventing erosion (Gupta & Dwivedi, 2023). (ii) Flow Stabilization: In a sloping expanding channel, the flow velocities are higher in the narrower sections and decrease as the channel expands. This variation in velocity can lead to flow

instabilities and turbulence. The hydraulic jump helps to stabilize the flow by providing a transition from a high-velocity, unstable flow to a lower-velocity, more stable flow (Parsaie et al., 2018; Kramer & Valero, 2020). (iii) Preventing Sediment Transport: Excessive flow velocity in a sloping channel can cause sediment erosion and transport. A hydraulic jump is created, which lowers the flow velocity, reducing the potential for sediment movement and deposition (Ebrahimiyan et al., 2021; Gupta & Dwivedi, 2024a). (iv) Flow Control: Hydraulic jumps allow for better control of the flow in sloping expanding channels. By adjusting the design and geometry of the channel, engineers can manipulate the position and characteristics of the hydraulic jump to optimize flow conditions for specific requirements, such as preventing erosion, enhancing mixing, or promoting aeration (Welahettige et al., 2017; Hamidnejad et al., 2023). (v) Recirculation: In certain flow scenarios, hydraulic jumps can create recirculation regions, where some of the fluid is trapped and circulates within the

NOMENCLATURE			
$A_1$	area before expansion	$M_2$	momentum rate in subcritical flow
$A_2$	area after expansion	$P_1$	hydrostatic force in supercritical flow
$b_1$	channel width before expansion	$P_2$	hydrostatic force in subcritical flow
$b_2$	channel width after expansion	$P_e$	pressure force due to gradual expansion
$B$	divergence ratio	$Q$	discharge through channel
$d_1$	sloped channel initial depth	$R^2$	coefficient of regression
$d_2$	sloped channel sequent depth	SVM	Support Vector Machine
$E_1$	specific energy of jump in supercritical flow	$V$	average flow velocity
$E_2$	specific energy of jump in subcritical flow	$V_1$	flow velocity before jump
$E_L$	loss of energy due to formation of jump	$V_2$	flow velocity after jump
$f$	function of	$W$	weight of water in jump
$Fr_1$	inflow Froude number	$Y_1$	horizontal channel supercritical flow depth
$g$	gravitational acceleration	$Y_2$	flow depth in horizontal channel after jump
$h$	height of roughness	$\rho$	mass density
$Re_1$	inflow Reynolds number	$\gamma$	weight density
$L_j$	hydraulic jump length	$\mu$	dynamic viscosity
$M_1$	momentum rate in supercritical flow	$\theta$	bed slope

jump's turbulent core. This phenomenon can be useful for specific mixing and transport applications (Chanson & Brattberg, 2000; Wang et al., 2023). (vi) Dissipation of Negative Surges: In certain scenarios, sudden changes in flow velocity in a sloping channel can lead to negative surges or backflows, causing pressure fluctuations and potential damage to the channel and downstream structures. Hydraulic jumps help to dissipate these negative surges, ensuring a smoother flow transition (Kim et al., 2015; Mnassri & Triki, 2023). (vii) Aeration and Oxygenation: Hydraulic jumps can also introduce air into the flow, promoting aeration and oxygenation of the water. This is beneficial for maintaining the health of aquatic ecosystems and improving water quality (Baylar et al., 2006; Kucukali & Cokgor, 2009). Hydraulic jumps are essential in sloping expanding channels to control flow velocities, prevent erosion, stabilize the flow, and manage energy dissipation. Properly designed hydraulic jumps contribute to the overall efficiency and sustainability of water management and engineering projects involving sloping channels.

Numerous scholars have been interested in hydraulic jumps with diverging portions. Rajaratnam and Subramanya (1968) performed experiments on a suddenly expanding horizontal channel, varying the expansion ratio from 0.3 to 0.9 and the inflow Froude number from 2 to 9, and developed an empirical correlation for the depth ratio, as represented by Eq. 1

$$\frac{Y_2}{Y_1} = (Fr_1 - 0.85) \left( \frac{1}{B_1/B_2} + 0.3 \right) + 0.75 \quad (1)$$

Another correlation for the depth ratio, represented by Eq. 2 in a suddenly expanding horizontal channel, was developed by Herbrand (1973) without considering bed friction. The experiments were conducted on six expansion ratios, which ranged from 0.288 to 1, and throughout the study, the Froude number ranged from 3.1 to 9.6. They concluded that, under the same inflow conditions, a hydraulic jump near a lateral enlargement produces a narrower stilling basin than a conventional hydraulic jump. The absence of appurtenances in the

temporal hydraulic jump tends to increase the volatility and asymmetry of the discharge, impairing energy dissipation and causing the tailwater to be dispersed unevenly.

$$\frac{Y_2}{Y_1} = \sqrt{\frac{2}{B_2/B_1} Fr_1 + \frac{B_1}{2B_2}} \quad (2)$$

Peterka (1958) developed correlation for relative energy loss and jump length in a suddenly expanding horizontal channel, represented by Eq. 3 and Eq. 4 respectively.

$$\frac{E_L}{E_1} = \frac{Y_1 - Y_2 + \frac{Fr_1^2 Y_1}{2} \left( 1 - \left( \frac{A_1}{A_2} \right)^2 \right)}{Y_1 + \frac{Fr_1^2 Y_1}{2}} \quad (3)$$

$$\frac{L_j}{Y_1} = 220 \left( \frac{e^z - e^{-z}}{e^z + e^{-z}} \right) \quad \text{where } z = \frac{Fr_1 - 1}{22} \quad (4)$$

Matin et al. (2008) conducted experiments on a suddenly expanding sloped rectangular channel to develop a correlation for the depth ratio, represented by Eq. 5, considering the effects of both channel slope and sudden expansion ratio. They concluded that when the tailwater condition is very low, this type of jump can be used as an energy dissipater.

$$D = \frac{1}{2} \left( \sqrt{1 + 8Er_1^2} - 1 \right) \quad (5)$$

Where D is the depth ratio  $Er_1$  is the modified Froude number which is represented as

$$Er_1^2 = \frac{Fr_1^2}{k_1(1 - k_2)\cos\theta} \quad (6)$$

Where  $k_1$  is the sudden expansion modification factor and  $k_2$  sloped channel modification factor. They also predicted the value of  $k_1$  and  $k_2$  through experimental observation.

Varaki et al. (2014) performed experimental research on adverse slopes with diverging channels. The findings

demonstrated that, compared to the conventional hydraulic jump, the relative energy loss increased by 20%, while the depth ratio and the relative jump length decreased by 47% and 35%, respectively, for each diverging angle. Furthermore, compared to the classic hydraulic jump, increasing the angle of divergence to 10 degrees reduced the depth ratio and the relative jump length by 51% and 38%, respectively, while increasing the relative energy loss by 23% for each negative bed slope. [Daneshfaraz et al. \(2017\)](#) carried out experimental study on both contraction and expansion channels with curved walls to investigate various hydraulic jump characteristics. During the experiment, the Froude number ranged from 5.8 to 9.1. The study's findings indicate that there was an average 8.74% decrease in energy dissipation during contraction compared to expansion. The findings also revealed that, for constant inflow Froude numbers, contractions produced longer secondary depths and jumps than expansions. The hydraulic jump formed during contraction lost less energy than that formed during expansion. [Chen et al. \(2013\)](#) conducted experiments on expanding channels following a free overfall to investigate energy dissipation. They found that hydraulic jumps in expanding channels experience greater energy loss, with the energy loss percentage rising as the channel expansion ratio increases. Additionally, the depth ratio decreases when a hydraulic jump occurs in an expanding channel with a higher expansion ratio, leading to a decrease in the tailwater height downstream. In an expanding channel, as opposed to a prismatic channel, hydraulic jump energy dissipation following a free overfall is higher. [Benmalek et al. \(2023\)](#) conducted experimental work on different basic shapes to predict energy dissipation in supercritical flow. Their results revealed that the efficiency of the trapezoidal channel could reach 85%, compared to 70% for the abruptly enlarged trapezoidal channel. However, the efficiency increased to 85% in the case of the compound rectangular channel. [Omid et al. \(2009\)](#) conducted a laboratory experiment in a trapezoidal channel to predict the behaviour of an expanding hydraulic jump. In their experiments, the Froude number ranged from 3 to 10, and the expansion angle varied between 30° and 90°. They found that the depth ratio and jump length were 30% and 22% lower, respectively, than those of a conventional hydraulic jump at a divergence angle of 90°. [Bremen and Hager \(1993\)](#) worked on abruptly expanding channels, focusing solely on T-jumps. Their findings revealed that the demands for compactness and symmetry of the jump are not met by an effective T-jump. Therefore, T-jumps lacking additional baffles and termination components are unsuitable for complete energy dissipation. [Zhang et al. \(2017\)](#) performed experimental research on the impact of expanding conjunctions on jump characteristics. They concluded that for a suddenly expanding tandem, a larger abrupt expansion ratio produces a smaller height after the formation of the jump, and this influence becomes more pronounced for larger ratios. For abrupt expansion ratios of 1.2, 1.4, and 1.5, the average decrement ratios were 6.57%, 7.68%, and 8.77%, respectively. [Elaswad et al. \(2022\)](#) predicted the performance of a screen on a

submerged hydraulic jump in a suddenly expanding channel through experimental observations. They used four relative distances, which varied from 0.25 to 1. They determined that the optimal relative position for the screen in the contracted section was at a screen length ratio of 0.25. For a Froude number of 4.50 and submergence ratios of 2.5, the relative energy loss increased by 30%, while the relative depth and jump length reduced by 35% and 40%, respectively, compared to the scenario without a screen. [Gul et al. \(2021\)](#) conducted experiments and modeled a hydraulic jump using a hybrid algorithm in a suddenly expanding channel. According to their findings, the tenth fold of the newly published experimental data in this study matched the folds of data previously described in the research literature quite well.

[Daneshfaraz et al. \(2020b\)](#) investigated the S-jump in basins with stilling, abrupt divergence, and irregular beds. According to their findings, the subsequent depth and jump length on the irregular bed decreased by 20% and 16%, respectively, compared to the smooth bed. When compared to the conventional jump, the energy dissipation in this type of channel increased by 23.5% and 28.7% for the smooth and irregular beds, respectively. [Daneshfaraz et al. \(2020a\)](#) investigated the dissipation of energy in the sudden contraction of supercritical flow both experimentally and numerically. The findings demonstrated that dissipation of energy increases as the Froude number rises. Additionally, the presence of a sudden contraction enhances energy loss due to the increased backwater profile and downstream flow depth. [Daneshfaraz et al. \(2021a\)](#) predicted the energy dissipation in suddenly expanding rough surfaces using the SVM technique. The findings demonstrate that energy dissipation increased as the Froude number grew for all roughness heights, and relative energy dissipation was selected as the optimal parameter after sensitivity analysis. [Daneshfaraz et al. \(2021b\)](#) examined the impact of bat-shaped features in an abruptly expanding channel. The findings showed that compared to a smooth rectangular channel, the shear stress in the coarse bed of an expanding conduit was more than twelve times higher. Furthermore, the rough bed exhibited a 22% reduction in secondary depth and a 9–13% shorter S-jump length compared to the smooth bed. [Daneshfaraz et al. \(2022\)](#) experimentally studied the hysteretic behavior of torrential flow near structures, focusing on channel width contractions. The study found that varying the flow rate resulted in two distinct flow behaviors under identical conditions. As the rate of sudden contraction increased, relative depths decreased, initially indicating a subcritical regime. In the secondary flow, hysteresis caused some discharges to shift to a supercritical regime.

[Maryami et al. \(2021\)](#) predicted various hydraulic jump characteristics using numerical and analytical techniques in a closed conduit. The findings demonstrate that, with an error of less than 5%, the numerical approach predicts the depth ratio after the conduit more accurately than the analytical method, which has an error of less than 10%. Furthermore, when the Froude number climbs from 4.617 to 5.562 at a slope of 0.00, energy loss rises by 16%. The energy loss rises by 23% and 22%,

**Table 1 Correlations developed by researchers on various jump characteristics**

Ref. No.	Type of Channel	Jump Characteristics Equation	R <sup>2</sup>
Varaki et al. (2014)	Diverging	$\frac{y_2}{y_1} = 0.309(S + 1)^{3.4542} (Fr_1^{0.5175})(L_j/y_1)^{0.5444} + 1.4396$ where S=tanφ	0.92
Varaki et al. (2014)	Diverging	$\frac{L_j}{y_1} = 2.9607(S + 1)^{3.7214} (\theta + 1)^{-0.0774} (Fr_1^{1.4997})$	0.95
Hassanpour et al. (2017)	Expanding	$\frac{d_2}{d_1} = 0.832Fr_1 + 1.998B - 1.250\left(\frac{h}{d_1}\right) - 0.432$	0.95
Hassanpour et al. (2017)	Expanding	$\frac{L_j}{d_1} = 8.924Fr_1 + 11.473B - 12.39\left(\frac{h}{d_1}\right) - 21.541$	0.89
Hassanpour et al. (2017)	Expanding	$\frac{E_L}{E_1} = 0.250 \ln(Fr_1) - 0.024B^2 - 0.023B + 0.026\left(\frac{h}{d_1}\right) + 0.244$	0.98
Torkamanzad et al. (2019)	Expanding	$\frac{d_2}{d_1} = 0.797(Fr_1) - 0.855\left(\frac{h}{d_1}\right) + 4.097(B) - 1.388$	0.962
Torkamanzad et al. (2019)	Expanding	$\frac{L_j}{d_1} = 9.833(Fr_1) - 87.568(B)^2 + 142.142(B) + 3.68\left(\frac{h}{d_1}\right)^2 - 14.635\left(\frac{h}{d_1}\right) - 54.58$	0.958
Torkamanzad et al. (2019)	Expanding	$\frac{E_L}{E_1} = 0.229 \ln(Fr_1) + 0.102(B)^2 - 0.267(B) + 0.021\left(\frac{h}{d_1}\right) + 0.408$	0.980
Abnavi et al. (2023)	Divergent-Convergent	$\frac{y_2}{y_1} = 2.352 + 0.517Fr_1 + 0.11\left(\frac{b}{y_1}\right) - 1.19\left(\frac{\theta_1}{\theta_2}\right)$	0.959
Abnavi et al. (2023)	Divergent-Convergent	$\frac{L_j}{y_1} = 13.69 + 0.496Fr_1 + 0.8\left(\frac{b}{y_1}\right) - 4.3\left(\frac{\theta_1}{\theta_2}\right)$	0.874
Abnavi et al. (2023)	Divergent-Convergent	$\frac{E_L}{E_1} = 0.3 + 0.086Fr_1 - 0.003(Fr_1^2) + 0.048\left(\frac{\theta_1}{\theta_2}\right)$	0.982

respectively, at slopes of 0.01 and 0.02. Sharoonizadeh et al. (2022) experimentally investigated various jump characteristics with a jet injection system in an expanding channel. After testing different jet system configurations using three Froude numbers (7.4, 8.7, and 9.5), arrangements 1, 2, and 3 were determined to be the three best options. Their results revealed that arrangement 3 had the greatest relative energy loss, which was 68.42%. Abnavi et al. (2023) investigated hydraulic jump in divergent-convergent (D-C) basins in horizontal channels in the laboratory. Comparing the D-C basin to the standard basin, they discovered that the jump length and depth ratio had dropped by 122.9% and 48.6%, respectively. Compared to traditional basins, the D-C basin showed a 26.8% increase in energy dissipation. The correlations developed by the researchers for various jump characteristics are presented in Table 1.

From the literature review, it was observed that hydraulic jumps in conventional rectangular channels were investigated in earlier research or with individual effects of slope or expansion. A few studies examined how channel slope and expansion ratio interact to affect hydraulic jump characteristics. Furthermore, the lack of generalized correlations for predicting jump parameters under these conditions represents a significant knowledge

gap. This study investigates the combined effects of channel slope and expansion ratio on hydraulic jump characteristics through extensive experimental analysis. Novel correlations were developed to predict depth ratio (d<sub>2</sub>/d<sub>1</sub>), relative energy loss (E<sub>L</sub>/E<sub>1</sub>), and relative jump length (L<sub>j</sub>/d<sub>1</sub>), addressing existing gaps in the literature. The findings provide valuable insights for optimizing water conveyance structures, contributing to sustainable water resource management.

The objective of the research is to advance scientific understanding of hydraulic jumps in suddenlyexpanding sloping channels while exploring their implications for achieving a sustainable environment. By addressing this objective, the study aims to contribute to more eco-friendly and efficient water management practices that can help protect the environment and foster sustainable development.

## 2. ANALYSIS OF GRADUALLY EXPANDING SLOPING CHANNEL HYDRAULIC JUMP

### 2.1 Analytical Analysis

Hydraulic jump characteristics in an expanding sloping channel have been analyzed analytically using a



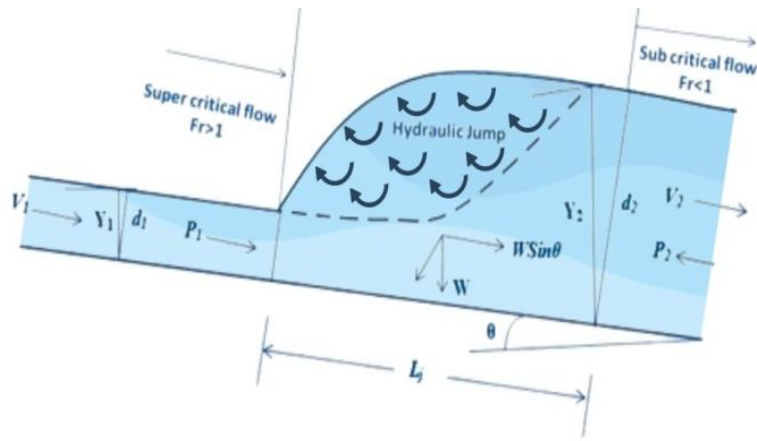


Fig. 1 Hydraulic jump formation in expanding sloping channel

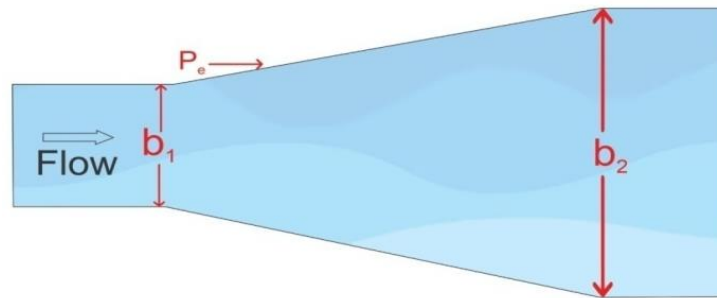


Fig. 2 Plan view of channel expansion

momentum equation between supercritical flow and subcritical flow, as shown in Fig. 1 and Fig. 2. All the effective forces acting are assumed to be parallel to the channel bottom. The generalized momentum equation for a gradually expanding sloping channel is given by Eq. 7. Many unknown terms are involved in the generalized momentum equation, so it is almost impossible to solve without experimental observation. The main challenge is to compute the water weight ( $W \sin \theta$ ) in the jump profile, as it incorporates both the jump profile and the length of the jump.

Energy loss increases due to an increase in channel expansion on sloping surfaces. It is because of more kinetic energy is converted into potential energy in the expanding channel. The momentum principle can be used to calculate the impact of channel expansion and all other hydraulic jump characteristics. The generalized momentum equation can be expressed as,

$$P_1 - P_2 + P_e + W \sin \theta = M_2 - M_1 \quad (7)$$

Where,

$$P_1 = \frac{1}{2} \gamma b_1 d_1^2 \cos \theta, P_2 = \frac{1}{2} \gamma b_2 d_2^2 \cos \theta, M_2 = \rho Q V_2, \\ M_1 = \rho Q V_1$$

The pressure force due to gradual expansion can be calculated as

$$P_e = \frac{1}{2} \gamma (b_2 - b_1) d_1^2 \cos \theta \quad (8)$$

Water weight in the jump profile can be calculated as Eq. 9 (Jan & Chang, 2019)

$$W = \frac{1}{2} \gamma b_2 L_j (d_1 + d_2) \quad (9)$$

Now the momentum equation can be represented as

$$\frac{1}{2} \gamma b_1 d_1^2 \cos \theta - \frac{1}{2} \gamma b_2 d_2^2 \cos \theta + \frac{1}{2} \gamma (b_2 - b_1) d_1^2 \cos \theta \\ + \frac{1}{2} \gamma b_2 L_j (d_1 + d_2) \sin \theta = \rho Q (V_2 - V_1) \quad (10)$$

Further, above equation is written as,

$$b_1 d_1^2 - b_2 d_2^2 + (b_2 - b_1) d_1^2 + b_2 L_j (d_1 + d_2) \tan \theta \\ = \frac{2Q}{g \cos \theta} (V_2 - V_1) \quad (11)$$

Using the continuity equation ( $b_1 d_1 V_1 = b_2 d_2 V_2$ ) and the concept of Froude number ( $Fr_1 = Q / \sqrt{g d_1^3 \cos \theta}$ ), the above momentum equation can be simplified as

$$\frac{d_2}{d_1} = 1 + \frac{L_j}{d_1} \tan \theta + \frac{2d_1 (V_1 - V_2)}{Fr_1^2 b_2 \left(1 + \frac{d_2}{d_1}\right)} \quad (12)$$

The specific energy in supercritical flow and subcritical flow can be evaluated by Eq. 13 and Eq. 14 as

$$E_1 = d_1 \cos \theta + \frac{V_1^2}{2g} + L_j \sin \theta \quad (13)$$

$$E_2 = d_2 \cos \theta + \frac{V_2^2}{2g} \quad (14)$$

The relative loss of energy which occurs due to the development of the jump can be calculated by Eq. 15 as below:

$$\frac{E_L}{E_1} = \frac{E_1 - E_2}{E_1} = \frac{(d_1 - d_2) + \frac{Fr_1^2 d_1}{2} \left( 1 - \left( \frac{A_1}{A_2} \right)^2 \right) + L_j \tan \theta}{d_1 \left( 1 + \frac{Fr_1^2}{2} \right)} \quad (15)$$

### 2.2 Methodology of Dimensional Analysis

The fundamental factors responsible for the jump phenomenon in an expanding sloping channel, are characterized as indicators mentioned in Eq. 16.

$$f(d_1, d_2, V_1, L_j, E_1, E_2, E_L, b_1, b_2, \rho, g, \mu, \theta) = 0 \quad (16)$$

A total of thirteen variables (dependent and independent) are present in the phenomenon, and the three basic dimensions of these variables are M, L, and T. According to Buckingham’s  $\pi$  theorem methodology, these variables are grouped into 10 dimensionless  $\pi$  terms, as represented by Eq. 17.

$$f_1(\pi_1, \pi_2, \pi_3, \pi_4, \pi_5, \pi_6, \pi_7, \pi_8, \pi_9, \pi_{10}) = 0 \quad (17)$$

$\rho, d_1, V_1$  are selected as repeating variables for this phenomenon according to the rules of  $\pi$  theorem analysis. Therefore, these  $\pi$ -terms can be represented by Eq. 18.

$$f_2 \left( \frac{d_2}{d_1}, \frac{L_j}{d_1}, \frac{E_L}{d_1 \cos \theta}, \frac{E_1}{d_1 \cos \theta}, \frac{E_2}{d_1 \cos \theta}, \frac{V_1^2}{gd_1 \cos \theta}, \frac{\rho V_1 d_1 \cos \theta}{\mu}, \frac{b_1}{d_1}, \frac{b_2}{d_1}, \theta \right) = 0 \quad (18)$$

From Buckingham’s  $\pi$  theorem methodology, it is observed that all jump characteristics such as depth ratio ( $d_2/d_1$ ), relative jump length ( $L_j/d_1$ ) and relative energy loss ( $E_L/E_1$ ) are the function of the inflow Froude number ( $Fr_1 = V_1/\sqrt{gd_1 \cos \theta}$ ), inflow Reynolds number ( $Re_1 = \rho V_1 d_1 \cos \theta/\mu$ ), channel slope ( $\theta$ ) and expansion ratio ( $B = b_1/b_2$ ). The expansion ratio ( $B = b_1/b_2$ ) is obtained by dividing a  $\pi$ - terms ( $b_1/d_1$ ) by another  $\pi$ -terms ( $b_2/d_1$ ) as per the rule of Buckingham’s  $\pi$  theorem. These relationships can be represented by Equation 19.

$$\frac{d_2}{d_1}, \frac{L_j}{d_1}, \frac{E_L}{E_1} = f_3(Fr_1, Re_1, B, \theta) \quad (19)$$

Since the Reynolds number fluctuates between 7150 and 27750, the flow is completely turbulent; therefore the effects of Reynolds number (viscous effect) can be neglected. This is consistent with prior literature on turbulent flow in hydraulic jump studies (Hager & Bremen, 1989; Murzyn & Chanson, 2008; Pourabdollah et al., 2022; Daneshfaraz et al., 2022).

The jump characteristics primarily depend on the inflow Froude number ( $Fr_1$ ), channel slope ( $\theta$ ), and expansion ratio ( $B = b_1/b_2$ ). The inflow Froude number

determines the jump’s strength by indicating flow inertia relative to gravity. The channel slope affects flow momentum and jump position, while the expansion ratio influences velocity distribution and pressure variations in the expanding channel.

Previous experimental and theoretical studies consistently show that these three parameters govern the energy dissipation, flow regime, and stability of hydraulic jumps in expanding channels (Varaki et al., 2014; Hassanpour et al., 2017; Daneshfaraz et al., 2020b; Abnavi et al., 2023). Thus all the jump characteristics can be expressed as a function of  $Fr_1, B$  and  $\theta$ , as shown in Eq. 20.

$$\frac{d_2}{d_1}, \frac{L_j}{d_1}, \frac{E_L}{E_1} = f_4(Fr_1, B, \theta) \quad (20)$$

### 3. EXPERIMENTAL METHODOLOGY AND INSTRUMENTATION

The laboratory experiments were carried out in the Fluid Mechanics and Channel Flow laboratory of G.L.A. University, Mathura. The experiments were performed in a channel having dimensions (3.5m length  $\times$  0.45m width  $\times$  0.50m depth). To ensure the steady flow situation in the working channel, a stilling basin of dimension (2.25m length  $\times$  0.45m width  $\times$  0.50m depth) was installed before the working section. A perspex sheet was used to visualize the hydraulic jump phenomenon. The schematic arrangement of the experimental setup, including a side view of the working section and an elevation view of the expanding section, is displayed in Fig. 3. The water is supplied from the reservoir to the supply tank having dimensions (3.7m length  $\times$  3.7m width  $\times$  3.2m depth) with the help of a centrifugal pump and connecting pipe having diameter 0.15m. A regulating valve, installed after the supply tank, is used to control the flow into the inlet tank, which has dimensions (0.5m length  $\times$  0.5 m width  $\times$  0.85m depth). The channel surface is made of cement to ensure even flow and minimize the formation of chaotic flow and eddies. A sluice gate installed at the starting position of the working channel regulates the inflow and controls the water level upstream of the gate, thereby regulating the flow rate downstream. An adjustable vertical controlling gate with blunt edges is positioned at both the top and bottom of the stilling flume to manage and control the flow depth into the working flume. The sluice gate also ensures that the flow depth in the supercritical flow condition is equal to the gate opening. Supercritical flow is generated in the channel by adjusting the sluice gate. A tailgate is installed after the expanding channel at the end of the working section. The tailgate is used to regulate and modify the toe position of the hydraulic jump in the expansion portion. The primary purpose of the tailgate is to manage the flow exiting the experimental setup and maintain a tranquil flow after the formation of the hydraulic jump. Water is finally collected in a discharge tank after being discharged from the working flume through the tailgate.

An ultrasonic flow meter with an accuracy range of 0.7% to 1% is used to measure the discharge in the

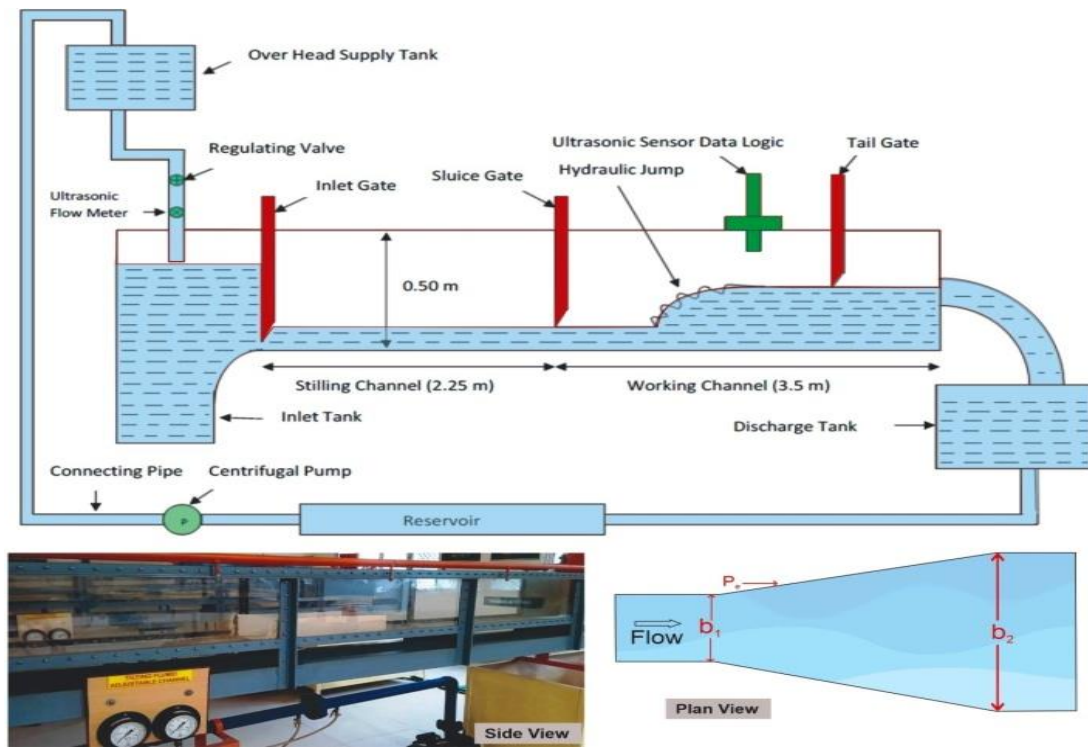


**Fig. 3 Schematic Layout of Experimental Set-up**

flume. To maintain a steady flow in the stilling basin and keep the Froude number constant, the flow level in the supply tank is kept steady and constant. After stabilizing the hydraulic jump in the working flume, the initial depth ( $d_1$ ), sequent depth ( $d_2$ ) and also depth at various positions of the working flume are measured with the help of an ultrasonic sensor (data logger US30) having accuracy of  $\pm 0.1$  mm. The sensor's operational range was 10 to 100 cm. Multiple measurement locations were used along the channel's length to account for the spatial variations in flow depth after the hydraulic jump. The ultrasonic sensor was carefully calibrated and positioned to capture consistent and precise depth measurements across these points. Although the measurements were primarily taken along the longitudinal axis of the flume, care was taken to ensure that the recorded depths represented the average depth across the flume width, as the flow in our setup remained relatively uniform laterally due to the design and boundary conditions of the channel. A ruler with  $\pm 1$ mm accuracy was positioned along the side wall of the conduit to measure the jump length.

The flow was ensured to be fully developed before the hydraulic jump by carefully designing the experimental setup and observing key flow characteristics. Specifically, a sufficiently long straight channel section was provided upstream of the working flume to allow the flow to stabilize and develop fully. This approach ensured that the velocity profile became uniform and the effects of upstream disturbances were minimized. Additionally, the flow was monitored using an ultrasonic sensor to measure depth variations along the channel. Consistent depth measurements and stable flow conditions along this section confirmed that the flow was fully developed before entering the expanding

and sloping channel sections where the hydraulic jump occurred.

The experiments were performed on four different channel slopes ( $0^\circ$ ,  $2^\circ$ ,  $4^\circ$ , and  $6^\circ$ ) and four distinct expansion ratios ( $B = b_1/b_2$ ) of 0.35, 0.45, 0.55 and 0.75. To accomplish the experiment on four different expansion ratios, four different models of expanding channels were built and installed in the working flume. For each gate opening, flow depth in supercritical and subcritical flow, lengths of the jump and volume flow rate were measured. For each set of experiments, 35 data were collected.

## 4. RESULT AND DISCUSSION

The laboratory assessment of hydraulic jump properties in a gradually expanding sloping channel yielded important information. Table 2 summarizes the experimental findings, highlighting the relationships between flow parameters. It was observed that the Froude number fluctuated between 2.5 and 8.5 during the course of the study, while the Reynolds number varied between 7,150 and 27,750. These variations underscore the influence of channel expansion and slope on jump behavior. The results offer valuable data for optimizing hydraulic structures under similar flow conditions.

### 4.1 Depth Ratio

The depth ratio of a hydraulic jump in a gradually expanding sloping channel represents the ratio of the downstream depth to the upstream depth, significantly influencing the jump's behavior and energy dissipation. It depends on various factors, including the channel's slope, expansion angle, upstream Froude number, and

**Table 2 Summary of experimental observation**

Experiment	$\theta$	B	$Fr_1$	$Re_1 \times 10^5$	$d_2/d_1$	$L_j/d_1$	$E_L/E_1$
1	0°	0.35	2.48-7.61	0.085823-0.231675	3.75-8.60	24.04-60.55	0.2520-0.8120
2	0°	0.55	2.47-7.62	0.087815-0.231867	4.24-9.08	27.72-63.06	0.2110-0.7613
3	0°	0.75	2.48-7.62	0.088156-0.230238	4.75-9.63	31.33-66.36	0.1669-0.7204
4	0°	1.00	2.49-7.57	0.088269-0.231793	5.28-10.01	33.41-69.14	0.1103-0.6702
5	2°	0.35	2.53-7.63	0.11493-0.25090	4.43-10.16	23.36-56.87	0.2914-0.8407
6	2°	0.55	2.55-7.66	0.11409-0.26207	4.88-10.61	26.17-59.58	0.2331-0.7931
7	2°	0.75	2.54-7.63	0.11575-0.24080	5.51-11.14	28.85-62.44	0.1802-0.7492
8	2°	1.00	2.58-7.61	0.11686-0.26203	6.10-11.50	31.54-64.95	0.1413-0.6924
9	4°	0.35	2.53-7.68	0.11840-0.26389	4.88-11.66	21.67-55.05	0.2887-0.8791
10	4°	0.55	2.53-7.65	0.11953-0.26799	5.34-12.12	24.34-57.94	0.2383-0.8304
11	4°	0.75	2.52-7.64	0.12548-0.26687	5.98-12.78	27.13-60.78	0.2023-0.7842
12	4°	1.00	2.56-7.62	0.12576-0.26673	6.61-13.30	29.92-63.24	0.1412-0.7206
13	6°	0.35	2.71-7.60	0.113753-0.27294	6.02-12.86	20.93-52.97	0.3379-0.9422
14	6°	0.55	2.71-7.59	0.113436-0.27698	6.47-13.38	23.38-55.24	0.2758-0.8896
15	6°	0.75	2.73-7.61	0.113309-0.27653	6.98-13.89	26.36-58.12	0.2304-0.8453
16	6°	1.00	2.73-7.62	0.1125789-0.27605	7.46-14.21	28.96-60.92	0.1704-0.7915

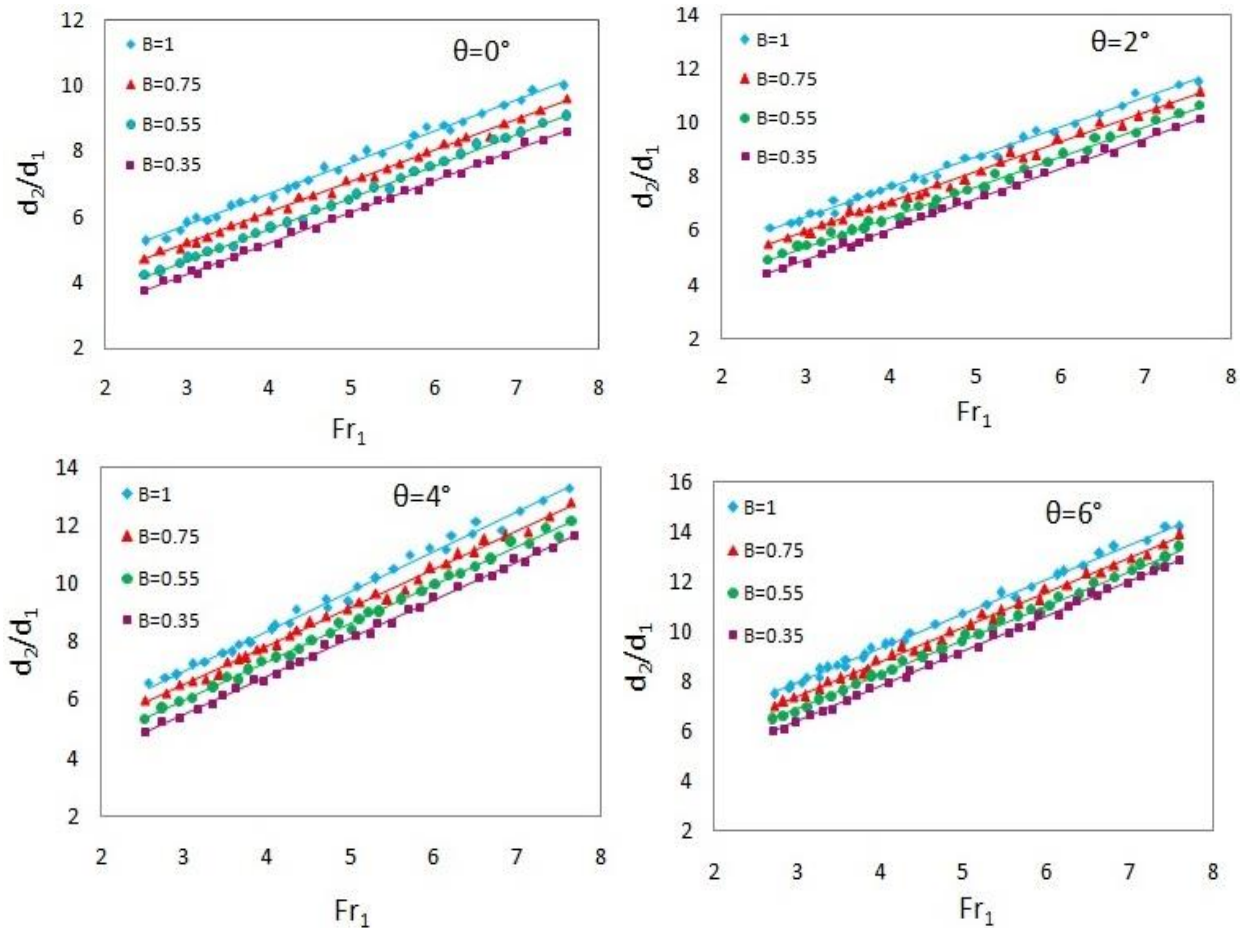


**Fig. 4 Variation of depth ratio ( $d_2/d_1$ ) with varying divergence ratio (B) and channel slope ( $\theta$ ) against inflow Froude number ( $Fr_1$ )**

flow velocity. In sloping channels, the interplay between gravitational forces and flow momentum alters the hydraulic jump characteristics, while the gradual expansion reduces flow velocity, promoting enhanced energy dissipation and stability of the jump (Daneshfaraz et al. 2019).

The observation derived from the examination of the  $\pi$

theorem and Eq. 20 indicates that the depth ratio ( $d_2/d_1$ ) depends on three parameters:  $Fr_1$ , B, and  $\theta$ . The plot showing the variation of the depth ratio ( $d_2/d_1$ ) with varying divergence ratio (B) and channel slope ( $\theta$ ) against the inflow Froude number ( $Fr_1$ ) is demonstrated in Fig. 4. Table 3 displays the average values of the depth ratio ( $d_2/d_1$ ) at distinct bed slopes and expansion ratios.



**Table 3 Average value of depth ratio ( $d_2/d_1$ ) at different channel slope and expansion ratio**

$\theta$	$d_2/d_1$ (B=1)	$d_2/d_1$ (B=0.75)	$d_2/d_1$ (B=0.55)	$d_2/d_1$ (B=0.35)
0°	7.512779	6.964322	6.491305	6.059118
2°	8.463886	7.944834	7.410000	6.972903
4°	9.551577	9.018081	8.698404	8.247759
6°	10.27419	10.06907	9.76500	9.42500

The depth ratio ( $d_2/d_1$ ) rises as inflow Froude number ( $Fr_1$ ), the expansion ratio (B), and bed slope ( $\theta$ ), all increase, as seen in Fig. 4. In other words, it is concluded that the depth ratio for an expanding channel is lower than that for a conventional hydraulic jump of the same size in a rectangular channel. It was also noted by Hassanpour et al. (2017) and Torkamanzad et al. (2019) that the depth ratio in an expanding horizontal channel varied similarly with the inflow Froude number. When the expansion ratio of the channel increases, it generally provides more space for energy dissipation and flow expansion during the hydraulic jump. This results in a more efficient slowing down of the flow velocity and greater energy dissipation, leading to a higher sequent depth relative to the critical depth. Consequently, when the expansion ratio rises, so does the hydraulic jump's depth ratio.

The relationship for the depth ratio among the variables, obtained from the  $\pi$ -theorem analysis for four divergence ratios, four channel slopes, and the inflow Froude number, can be represented by the experiment-based regression Eq. 21, with a regression coefficient ( $R^2$ ) of 0.9955.

$$\frac{d_2}{d_1} = 1.39Fr_1^{0.92} + 24 \tan \theta + 1.825(B) + 0.047 \quad (21)$$

From Eq. 21, it is observed that the depth ratio ( $d_2/d_1$ ) increases as inflow Froude number ( $Fr_1$ ), the expansion ratio (B), and bed slope ( $\theta$ ) increase. The comparative plot of the average depth ratio in a sloping channel at various expansion ratios is shown in Fig. 5.

It is observed from Fig. 5 that the depth ratio ( $d_2/d_1$ ) reduces with a decrement in the expansion ratio. A hydraulic jump occurs when the flow changes from a torrential, high-velocity flow to a tranquil, low-velocity flow. The jump occurs due to the transformation of the energy of motion into potential and internal energy, resulting in a sudden increase in water depth and energy dissipation. When the expansion ratio of the channel is decreased, the hydraulic jump experiences a more abrupt transition from the higher-velocity flow to the lower-velocity flow. This abrupt transition requires a higher degree of energy dissipation. The water slows down more quickly as it moves from the narrower section to the wider section, causing a greater loss of kinetic energy and resulting in a decrease in water depth after the jump. Consequently, the depth ratio ( $d_2/d_1$ ) decreases when the expansion ratio decreases.

The depth ratio ( $d_2/d_1$ ) in an expanding sloping channel increases with a rise in  $\theta$  and  $Fr_1$  due to the combined effects of gravitational forces, flow momentum, and energy dissipation. As the bed slope rises,

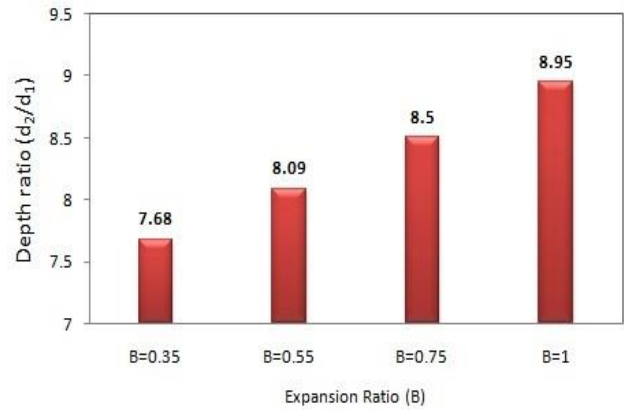


**Fig. 5 Comparative plot of the average value of depth ratio in the sloping channel at various expansion ratios**

the weight component along the flow direction intensifies, contributing to greater flow acceleration and an increase in downstream velocity. This leads to a more pronounced hydraulic jump, with a larger difference between the sequent depth ( $d_2$ ) and initial depth ( $d_1$ ). Additionally, a higher slope increases the energy dissipation capacity of the hydraulic jump, which promotes a more substantial rise in the downstream depth ( $d_2$ ). Likewise, a greater and more turbulent jump results from the kinetic energy of the incoming flow becoming more significant as the  $Fr_1$  rises. The additional turbulence and mixing associated with a higher  $Fr_1$  lead to enhanced energy dissipation, causing a greater increase in the downstream depth. These combined effects of slope and inflow Froude number highlight the interdependence of channel geometry and flow dynamics in shaping the behavior of hydraulic jumps.

Figure 6 presents a comparison plot between the depth ratios ( $d_2/d_1$ ) computed using Eq. 21 and the values measured during the current investigation. The results indicate an approximately  $\pm 10\%$  variance between the calculated data and the corresponding measured data, with an  $R^2$  value of 0.993, closely aligning with the regression agreement line. The findings demonstrate excellent efficacy and reliability in calculating the depth ratio using Eq. 21.

Depth deficit was described by Ead and Rajaratnam (2002) as  $d = (d_2^* - d_2)/d_2^*$ , which stands for the deficit of subsequent depth. Here,  $d_2^*$  denotes the sequent depth in the horizontal channel following a jump while taking into account the identical upstream conditions. Table 4 displays the average depth deficit percentage for all channel slopes and divergence ratios. It has been

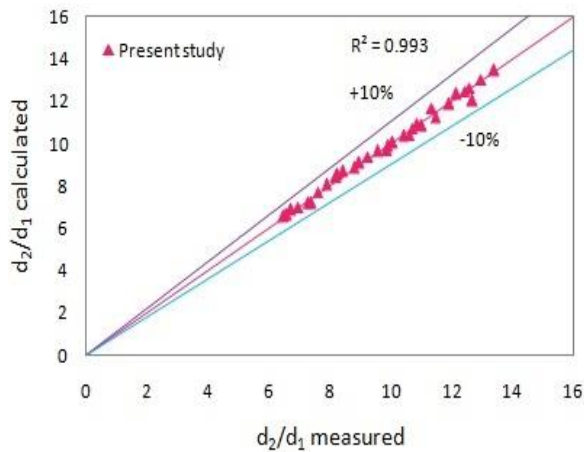


**Fig. 6** Comparative plot between measured and calculated value of depth ratio ( $d_2/d_1$ ) in expanding sloping channel

**Table 4** The average depth deficit ( $d$ ) % at various channel slopes and divergence ratios

Channel Slope ( $\theta$ )	B=1	B=0.75	B=0.55	B=0.35
0	0	7.53	14.17	20.06
2	-12.66	-5.75	1.37	7.19
4	-27.14	-20.03	-15.78	-9.78
6	-36.76	-34.03	-29.98	-24.45

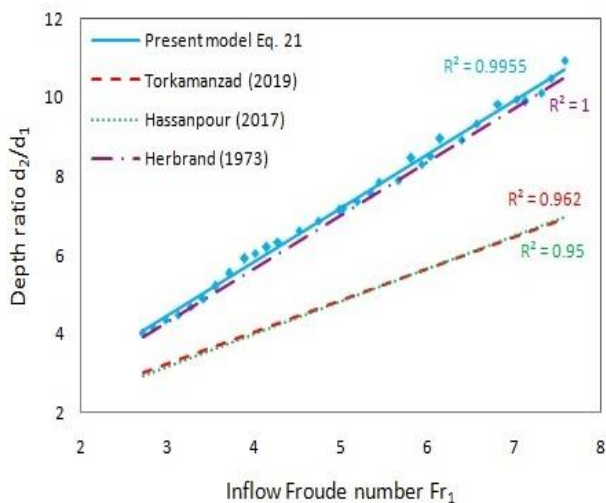


**Fig. 7** Comparison of correlation Eq. 21 with previously developed correlations of depth ratio

discovered that the percentage depth deficit reduces as the channel slope and divergence ratio rise. At a divergence ratio of 0.35 and channel slope  $0^\circ$ , the maximum depth deficit was discovered to be 20.06%.

Figure 7 presents a comparison plot of correlation Eq. 21 with previously developed correlations for the depth ratio by Herbrand (1973), Hassanpour et al. (2017), and Torkamanzad et al. (2019). It is observed that the correlations developed by Hassanpour et al. (2017) and Torkamanzad et al. (2019) nearly overlap, with  $R^2$  values of 0.95 and 0.962, respectively. The present correlation, Eq. 21, with an  $R^2$  value of 0.9955, is very close to the

correlation developed by Herbrand (1973), which has an  $R^2$  value of 1. This demonstrates excellent fitting and consistency of the present correlation Eq. 21.

The developed correlation of the depth ratio ( $d_2/d_1$ ) provides a valuable tool for understanding and predicting hydraulic jump behavior in gradually expanding sloping channels, making it highly relevant for optimizing the efficiency and sustainability of water conveyance structures. By incorporating key parameters such as channel slope ( $\theta$ ), expansion ratio (B), and inflow Froude number ( $Fr_1$ ), the correlation enables precise estimation of the downstream flow depth. This information is critical for designing channels and energy dissipation structures to ensure proper flow regulation, prevent erosion, and minimize structural damage. Moreover, the ability to predict depth ratio accurately allows engineers to optimize channel geometries, reducing material and construction costs while enhancing hydraulic performance. Additionally, the correlation supports the development of eco-friendly systems by enabling designs that reduce energy losses and environmental impacts. Thus, the correlation directly contributes to achieving sustainable water resource management and improving the overall efficiency of water conveyance systems.

#### 4.2 Relative Length of Jump

The relative jump length has a direct impact on how much energy dissipates in the flow. A longer jump length indicates greater energy loss, which can be beneficial for scenarios where reducing flow energy is necessary to prevent erosion, control water velocities, and avoid damage to structures downstream (Azimi et al., 2018b). Sudden changes in flow velocity and energy can have ecological implications in aquatic ecosystems. A longer relative jump length may create smoother transitions in water velocities, reducing the potential harm to aquatic organisms (Azimi et al., 2018a). The jump length can affect the design of infrastructure downstream of the jump. For example, bridges, culverts, and embankments must be designed to handle the altered flow conditions after the jump. It is difficult to quantify the hydraulic jump's length due to the surface wave (Carollo et al., 2012). Relative roller length and relative jump length are roughly identical, according to the majority of researchers. (McCorquodale & Mohamed, 1994; Roushangar & Homayounfar, 2019).

The analysis of the  $\pi$ -theorem and Eq. 20 revealed that  $L_j/d_1$  depends on three variables:  $Fr_1$ , B, and  $\theta$ . Figure 8 display the variation of  $L_j/d_1$  versus  $Fr_1$  while altering the divergence ratio (B) and channel slope ( $\theta$ ). The average  $L_j/d_1$  for various channel slopes and expansion ratios is shown in Table 5. The relative length of the jump ( $L_j/d_1$ ), as depicted in Fig. 8, increases with rising expansion ratio (B) and inflow Froude number ( $Fr_1$ ) but decreases with increasing channel slope ( $\theta$ ). Additionally, it was observed that an expanding channel exhibited a lower relative length of jump compared to a standard hydraulic jump in a rectangular channel of the same dimensions. Similar variations in the relative length of jumps with incoming Froude numbers on an expanding horizontal channel were also reported by Abnavi et al. (2023), Hassanpour et al. (2017), and Torkamanzad et al. (2019).

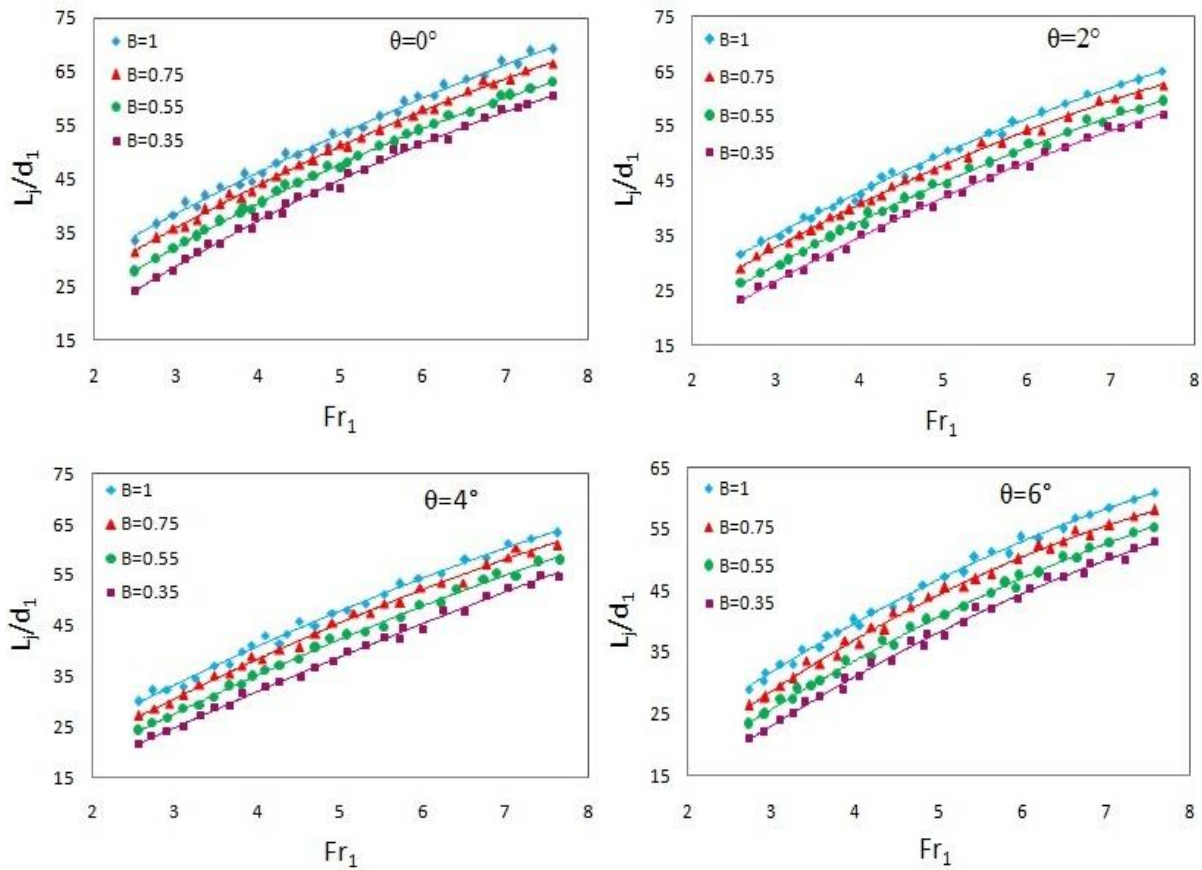


**Fig. 8** Variation of the relative length of jump ( $L_j/d_1$ ) with varying divergence ratio ( $B$ ) and channel slope ( $\theta$ ) against inflow Froude number ( $Fr_1$ )

**Table 5** Average value of relative length of jump ( $L_j/d_1$ ) at different channel slope and expansion ratio

$\theta$	$L_j/d_1$ ( $B=1$ )	$L_j/d_1$ ( $B=0.75$ )	$L_j/d_1$ ( $B=0.55$ )	$L_j/d_1$ ( $B=0.35$ )
$0^\circ$	45.25	49.73	46.43	43.49
$2^\circ$	47.46	45.22	43.01	41.05
$4^\circ$	46.05	43.33	41.12	38.55
$6^\circ$	47.71	45.49	42.45	40.27

In narrower channels with lower expansion ratios, the flow is forced to constrict, which can accelerate the flow velocity. Consequently, the flow must transition from supercritical to subcritical conditions more rapidly, resulting in a shorter hydraulic jump length.

The relationship for  $L_j/d_1$  among the variables derived from the  $\pi$ -theorem analysis for four divergence ratios, four channel slopes, and inflow Froude number can be represented by the experiment-based regression Eq. 22, which has a regression coefficient  $R^2$  of 0.991.

$$\frac{L_j}{d_1} = 8.34Fr_1^{0.85} - 50 \tan \theta + 17.348(B) + 2.953 \quad (22)$$

According to Eq. 22, the expansion ratio ( $B$ ) and the inflow Froude number ( $Fr_1$ ) increase the relative length of the jump ( $L_j/d_1$ ), whereas the channel slope ( $\theta$ ) reduces it. Fig. 9 presents a comparison plot of the average values of  $L_j/d_1$  in a sloping channel at various expansion ratios.

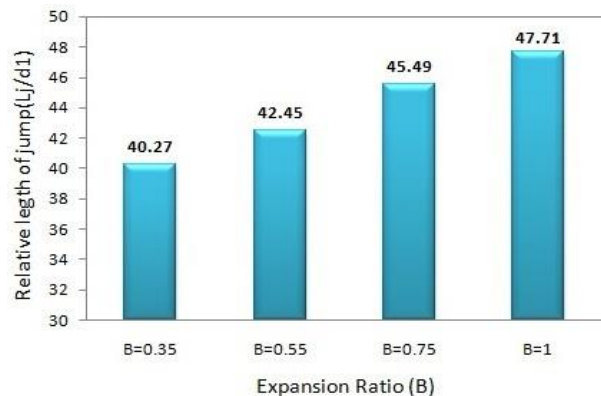


**Fig. 9** Comparative plot of the average value of the relative length of jump in the sloping channel at various expansion ratios

Figure 9 shows that as the expansion ratio in the sloping channel lowers,  $L_j/d_1$  also reduces. If there is a significant expansion ratio, it means that the flow area



after the jump is significantly greater than the flow area before the jump. In such cases, the hydraulic jump tends to be more gradual and elongated. The  $L_j/d_1$  is relatively long compared to the characteristic length of the channel. The jump is typically weaker, and the energy dissipation is spread out over a longer distance. The rate at which energy is lost during the hydraulic jump is directly related to the expansion ratio. For channels with lower expansion ratios, energy is dissipated more quickly due to the rapid transition, resulting in a shorter jump length. In a channel where the expansion ratio is smaller, the flow tends to have a higher Froude number before the jump due to the confined cross-sectional area. This means the flow is faster and more supercritical, leading to a shorter hydraulic jump length.

The relative length of jump ( $L_j/d_1$ ) in a hydraulic jump within an expanding sloping channel exhibits distinct behavior under the influence of the inflow Froude number ( $Fr_1$ ) and channel slope ( $\theta$ ) due to the interplay of flow energy and momentum. A greater and more powerful turbulent hydraulic jump results from the kinetic energy and momentum of the incoming flow becoming more significant as  $Fr_1$  rises. This heightened turbulence and energy dissipation require a longer distance for the flow to transition from supercritical to subcritical conditions, thereby increasing the relative jump length ( $L_j/d_1$ ). Conversely, as the bed slope ( $\theta$ ) rises, the weight component along the slope enhances the flow's downstream velocity and reduces the resistance to flow deceleration. This results in a more compact hydraulic jump, where the transition between flow regimes occurs over a shorter distance, leading to a decrease in the relative jump length. Additionally, the increased slope promotes more efficient energy dissipation within a shorter length, further contributing to the reduction in  $L_j/d_1$ . This behavior highlights the combined effects of flow dynamics and channel geometry on the characteristics of hydraulic jumps in expanding sloping channels.

Using Eq. 22,  $L_j/d_1$  is computed and plotted against the values from the present experiment in Fig. 10. The findings show that the computed data and corresponding measured data, which have an  $R^2$  value of 0.993 and are close to the regression agreement line, differ by approximately  $\pm 10\%$ . The results demonstrate high accuracy and consistency in calculating the  $L_j/d_1$  using Eq. 22.

The developed correlation for the  $L_j/d_1$  provides a practical framework for optimizing the efficiency and sustainability of water conveyance structures by offering a reliable method to predict the spatial extent of hydraulic jumps in expanding sloping channels. By incorporating critical parameters such as  $Fr_1$ ,  $\theta$ , and  $B$ , the correlation enables engineers to determine the precise length required for energy dissipation within the channel. This is essential for designing appropriately sized stilling basins and ensuring that the hydraulic jump remains confined within designated energy dissipation zones, preventing structural damage and erosion downstream. Furthermore, the correlation aids in reducing material and construction costs by avoiding overdesign while

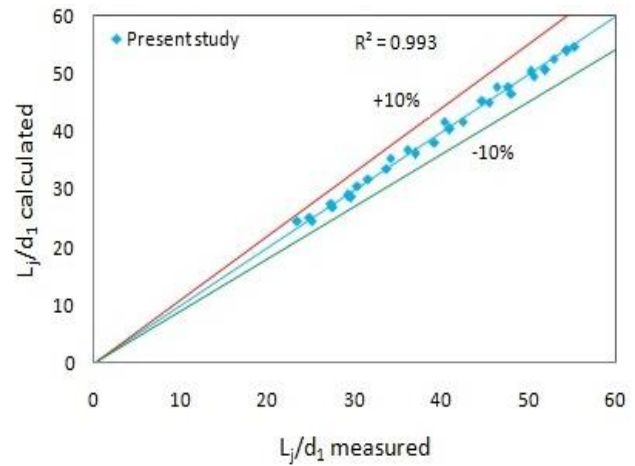


**Fig. 10 Comparative plot between measured and calculated value of relative length of jump ( $L_j/d_1$ ) in expanding sloping channel**

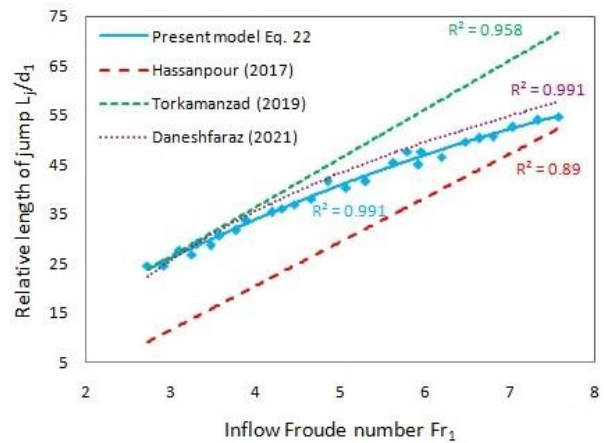


**Fig. 11 Comparison of correlation Eq. 22 with previously developed correlations of the relative length of the jump**

ensuring effective flow control. From a sustainability perspective, optimizing the jump length minimizes unnecessary energy loss and turbulence, contributing to eco-friendly designs that reduce environmental impacts. Therefore, the developed correlation serves as a key tool in balancing hydraulic performance, cost efficiency, and environmental considerations in water management systems.

Figure 11 presents the comparison plot of correlation Eq. 22 with previously developed correlations of  $L_j/d_1$  by Hassanpour et al. (2017), Torkamanzad et al. (2019), and Daneshfaraz et al. (2021b) using the data from the present study. It is observed that the correlation developed by Torkamanzad et al. (2019), with an  $R^2$  value of 0.958, is close to the present model (Eq. 22) and Daneshfaraz et al. (2021b) correlation at the beginning but diverges significantly at the end. In contrast, Hassanpour et al. (2017) model, with an  $R^2$  value of 0.89, is closer to the present model (Eq. 22) and Daneshfaraz et al. (2021b) at the end. The present model (Eq. 22), with an  $R^2$  value of 0.991, is much closer to the Daneshfaraz et al. (2021b) model, which also has an  $R^2$



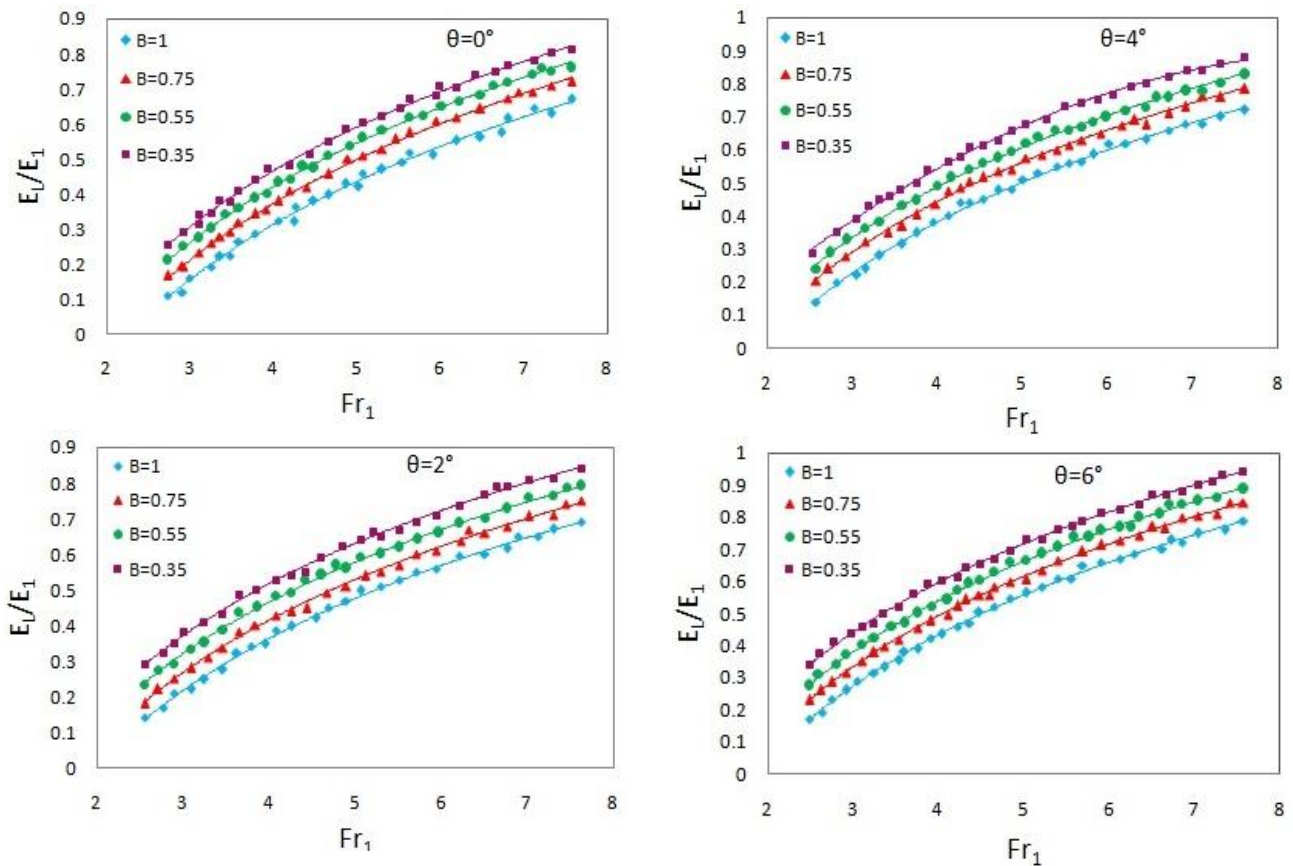


**Fig. 12** Variation of relative loss of energy ( $E_L/E_1$ ) with varying divergence ratio ( $B$ ) and channel slope ( $\theta$ ) against inflow Froude number ( $Fr_1$ )

value of 0.991. This demonstrates the excellent fitting and efficacy of the present correlation (Eq. 22).

### 4.3 Relative Loss of Energy

Engineers apply the concept of relative energy loss to design hydraulic structures like spillways, weirs, and stilling basins. Proper energy dissipation is crucial to prevent structural damage and maintain the integrity of these structures during high-flow events (Gupta & Dwivedi, 2024b). The importance of relative energy loss or energy dissipation in expanding channel hydraulic jumps lies in its ability to stabilize flows, prevent erosion, manage sediment transport, optimize energy recovery, control backwater effects, and enhance aquatic habitats (Mohammadzadeh-Habili et al., 2018; Daneshfaraz et al., 2023).

The logarithmic variation in the relative loss of energy ( $E_L/E_1$ ) with  $Fr_1$ , varying divergence ratio ( $B$ ), and channel slope ( $\theta$ ) is presented in Fig. 12. It is observed from Fig. 12 that  $E_L/E_1$  rises with the rise in  $Fr_1$  and  $\theta$ , and also increases with the decrease in divergence ratio ( $B$ ). A similar variation of  $E_L/E_1$  with  $Fr_1$  on an expanding horizontal channel was also shown by Hassanpour et al. (2017) and Torkamanzad et al. (2019). It was also demonstrated that an expanding channel dissipates energy more quickly than a typical hydraulic jump on a rectangular channel of the same size. The average value of  $E_L/E_1$  for various channel slopes and expansion ratios is shown in Table 6. In channels with smaller expansion ratios, there may be less flow separation and fewer

**Table 6** Average value of relative loss of energy ( $E_L/E_1$ ) at different channel slope and expansion ratio

$\theta$	$E_L/E_1$ ( $B=1$ )	$E_L/E_1$ ( $B=0.75$ )	$E_L/E_1$ ( $B=0.55$ )	$E_L/E_1$ ( $B=0.35$ )
$0^\circ$	0.403992	0.45634593	0.526666	0.556592
$2^\circ$	0.442759	0.50314175	0.548891	0.598618
$4^\circ$	0.47964	0.53901804	0.590785	0.633131
$6^\circ$	0.508201	0.57548202	0.626696	0.680756

recirculation zones in the jump region. Flow separation and recirculation zones can create additional turbulence and frictional losses, contributing to energy dissipation. The abrupt transition in flow conditions in a hydraulic jump with a smaller expansion ratio leads to more intense turbulence generation. The rapid deceleration of the flow can result in greater turbulence, which, in turn, leads to higher energy dissipation.

To represent the relationship for  $E_L/E_1$  among the variables obtained from the analysis of the  $\pi$ -theorem for the four divergence ratios, channel slopes, and the inflow Froude number, the experiment-based regression Eq. 23, with a regression coefficient  $R^2$  equal to 0.998, can be used.

$$\frac{E_L}{E_1} = 0.45 \ln(Fr_1^{0.85}) + 6 \tan \theta - 0.082(B) - 0.542 \quad (23)$$

Eq. 23 shows that  $E_L/E_1$  grew as  $Fr_1$  ascended logarithmically, as well as growing as the channel's

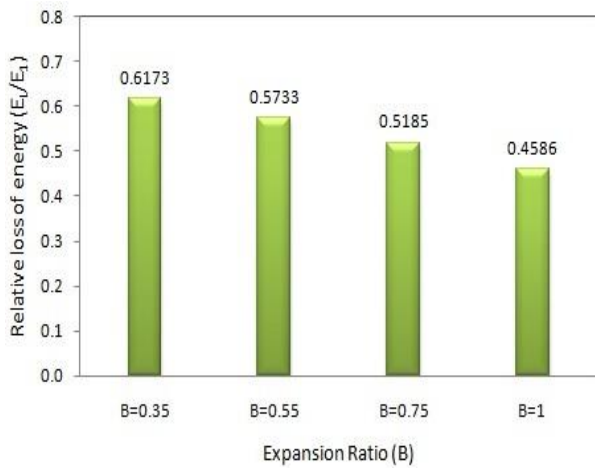


**Fig. 13** Comparative plot of the average value of relative loss of energy in the sloping channel at various expansion ratios

slope, but reduced when divergence ratio increased. With a higher Froude number, the flow has greater momentum, and this momentum must be reduced significantly during the hydraulic jump. As the flow transitions from supercritical to subcritical, there is a substantial reduction in momentum, resulting in a higher energy loss. In a hydraulic jump, the abrupt deceleration of the flow causes turbulence and mixing. Turbulence consumes energy through the generation of eddies and vortices. With a higher Froude number, the flow undergoes a more abrupt change in velocity, leading to more intense turbulence and energy dissipation. Along with a change in flow velocity, the hydraulic jump in an inclined channel also entails a change in flow depth. When the Froude number is high, the flow has more vertical displacement to undergo to reach the subcritical depth. This vertical displacement requires additional energy to be lost as the flow adjusts to the new depth.

$E_L/E_1$  rises with a rise in channel slope ( $\theta$ ) due to the enhanced gravitational influence and flow dynamics associated with steeper slopes. As  $\theta$  increases, the weight component along the slope intensifies, resulting in higher flow velocities downstream. The hydraulic jump becomes greater and more turbulent as a result of this increased velocity, where a greater portion of the initial energy ( $E_1$ ) is dissipated through turbulence, mixing, and flow resistance. Additionally, the steeper slope promotes a more abrupt change in flow from torrential to tranquil, further amplifying energy dissipation within the hydraulic jump. The increased energy loss is crucial for stabilizing flow and preventing erosion or damage to downstream structures. This behavior highlights the role of channel slope in enhancing energy dissipation efficiency, which is a key consideration in the design of hydraulic structures.

Figure 13 displays a comparison plot of the average value of  $E_L/E_1$  in a sloping channel at various expansion ratios (B). It can be observed from Fig. 13 that  $E_L/E_1$  in the sloped channel increased with a decrement in the expansion ratio. When the expansion ratio is small, the change in flow from torrential to tranquil is more abrupt,

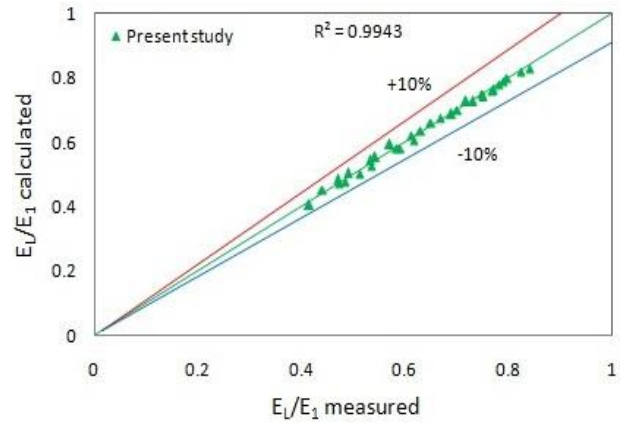


**Fig. 14** Comparative plot between measured and calculated value of relative loss of energy ( $E_L/E_1$ ) in expanding sloping channel

leading to greater turbulence. The turbulence causes energy dissipation through the conversion of kinetic energy into heat and internal energy, resulting in a higher energy loss. In hydraulic jumps, waves are generated at the boundary between supercritical and subcritical flow. When the expansion ratio is small, the waves tend to be steeper and more pronounced. These waves carry energy away from the main flow and dissipate it, contributing to higher energy losses. As water transitions from supercritical to subcritical flow, vortices are often formed in the recirculation zone downstream of the jump. These vortices enhance energy dissipation through turbulence and flow separation, particularly when the expansion ratio is small. A smaller expansion ratio depicts that there is less space for the flow to gradually decelerate and mix. This results in a more sudden and intense mixing of water, causing greater energy loss through the conversion of motion energy into potential energy and heat. This is why hydraulic engineers often aim to design hydraulic structures with appropriate expansion ratios to optimize energy losses and ultimately optimize the performance of the system.

In Fig. 14, a comparison plot is displayed between the results of the current experiment and the relative loss of energy ( $E_L/E_1$ ) estimated using Eq. 23. The results demonstrate a  $\pm 10\%$  difference between the computed data and the corresponding measured data, which had an  $R^2$  value of 0.9943 and were around the line of regression agreement. The results show that Eq. 23 can be used to calculate  $E_L/E_1$  with high accuracy and consistency.

Figure 15 represents the comparison plot of correlation Eq. 23 with previously developed correlations of relative loss of energy by Hassanpour et al. (2017), Torkamanzad et al. (2019) and Daneshfar et al. (2021b) using the data from the current investigation. It is observed that all the developed correlations of relative loss of energy have similar logarithmic variation with inflow Froude number having correlation coefficient  $R^2$  values of 0.998, 0.98, 0.98 and 0.974 respectively. From this, it is clear that present correlation Eq. 23 has the highest value of correlation coefficient which demonstrates how

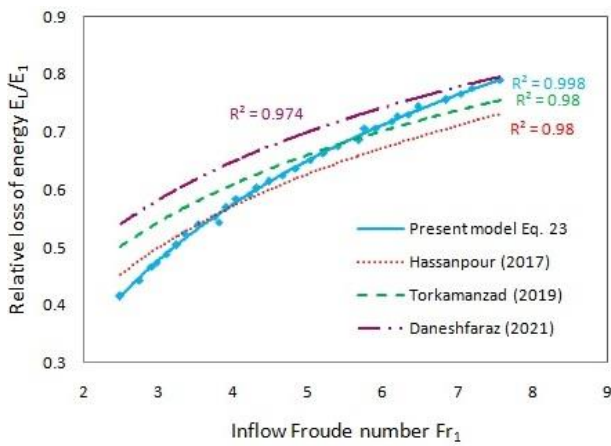


**Fig. 15 Comparison of correlation Eq. 23 with previously developed correlations of relative loss of energy**

effectively and well the current correlation Eq. 23 fits data.

The developed correlation for the relative loss of energy ( $E_L/E_1$ ) is directly tied to optimizing the efficiency and sustainability of water conveyance structures by enabling accurate prediction of energy dissipation in hydraulic jumps. By integrating factors such as channel slope ( $\theta$ ), expansion ratio ( $B$ ), and inflow Froude number ( $Fr_1$ ), the correlation provides insights into how different geometric and flow conditions influence energy loss. This is critical for designing effective energy dissipation systems, such as stilling basins, which prevent excessive downstream velocities that can lead to erosion or structural damage. By optimizing the energy dissipation process, the correlation helps in reducing unnecessary turbulence and energy inefficiencies, thereby improving the overall performance of the system. From a sustainability perspective, the correlation supports eco-friendly designs by minimizing the environmental impact of water conveyance systems, ensuring that flow transitions are controlled and safe for both infrastructure and surrounding ecosystems. Thus, the developed correlation serves as a key tool for achieving balance between hydraulic performance, cost-efficiency, and environmental stewardship.

#### 4. CONCLUSIONS

The research reveals a significant influence of channel slope and expansion ratio on hydraulic jump characteristics. The study demonstrates that altering the slope of the channel can lead to variations in jump characteristics. This knowledge is essential for optimizing channels and water management systems to ensure sustainable environmental practices. As the expansion ratio varies, it affects the flow patterns, energy dissipation, and hydraulic parameters of the jump. Understanding this relationship is crucial for designing hydraulic structures. The following are significant findings from this study:

The depth ratio ( $d_2/d_1$ ) increased by 13.93%, 31.41% and 46.27% as the channel slope rose to  $2^\circ$ ,  $4^\circ$  and  $6^\circ$

respectively, across all expansion ratios ranging from 0.35 to 1 while it decreased approximately by 5.04%, 9.60% and 14.24% with a decrement in expansion ratio 0.75, 0.55 and 0.35 respectively for all channel slope. The average increment in the depth ratio ( $d_2/d_1$ ) was 30.53% with an increment of channel slope from  $0^\circ$  to  $6^\circ$  for all expansion ratios while the average decrement depth ratio ( $d_2/d_1$ ) was 9.63% with a decrement of expansion ratio from 1 to 0.35 for all channel slopes. In comparison to a conventional jump, the depth ratio ( $d_2/d_1$ ) rises by 31.55% with a  $6^\circ$  increase in channel slope in the expanding channel.

The  $L_j/d_1$  drops by 7.90%, 11.39% and 14.04% as the channel slope rose to  $2^\circ$ ,  $4^\circ$  and  $6^\circ$  respectively, across all expansion ratios ranging from 0.35 to 1 and it also decrease by 4.64%, 11.01% and 15.60% with a decrement in expansion ratio 0.75, 0.55 and 0.35 respectively for all channel slope. The average decrement relative jump length ( $L_j/d_1$ ) was 11.11% with an increment of channel slope from  $0^\circ$  to  $6^\circ$  for all expansion ratios while the average decrement relative jump length ( $L_j/d_1$ ) is 10.42% with a decrement of expansion ratio from 1 to 0.35 for all channel slope. In comparison to a conventional jump, relative jump length ( $L_j/d_1$ ) decreases by 21.07% with a  $6^\circ$  increase in channel slope in the expanding channel.

The relative loss of energy ( $E_L/E_1$ ) increases by 7.71%, 15.38% and 23.03% as the channel slope rose to  $2^\circ$ ,  $4^\circ$  and  $6^\circ$  respectively, across all expansion ratios ranging from 0.35 to 1 and it also rises approximately by 13.05%, 24.99% and 34.59% with a decrement in expansion ratio 0.75, 0.55 and 0.35 respectively for all channel slope. The average increment in a relative loss of energy ( $E_L/E_1$ ) was 15.37% with an increment of channel slope from  $0^\circ$  to  $6^\circ$  for all expansion ratios and the average increment in a relative loss of energy ( $E_L/E_1$ ) was 24.21% with a decrement of expansion ratio from 1 to 0.35 for all channel slope. In comparison to a conventional jump, relative loss of energy ( $E_L/E_1$ ) rises by 47.97% with a  $6^\circ$  increase in channel slope in the expanding channel.

The findings of this research offer practical applications for hydraulic engineers and designers. Understanding, how can expansion ratio and channel slope affect hydraulic jumps help engineers design more efficient and environmentally friendly hydraulic structures, such as spillways and energy dissipation systems. Incorporating the knowledge gained from this study into hydraulic system design can lead to more sustainable practices. By optimizing the expansion ratio and channel slope hydraulic systems can operate with reduced environmental impact, aligning with the overarching goal of sustainable environmental management such as minimising erosion, sediment transport, and habitat disruption downstream, contributing to the protection and preservation of natural ecosystems.

#### CONFLICT OF INTEREST

The authors have no conflicts to disclose.



## AUTHORS CONTRIBUTION

**Sanjeev Kumar Gupta:** Conceptualization; methodology; formal analysis; writing original draft.  
**Vijay Kumar Dwivedi:** Review and editing of the manuscript

## REFERENCES

- Abnavi, M. H. J., Mohammadpour, R., & Beirami, M. K. (2023). Laboratory investigation of hydraulic jump in divergent-convergent conversions. *Flow Measurement and Instrumentation*, 94, 102444. <https://doi.org/10.1016/j.flowmeasinst.2023.102444>
- Azimi, H., Bonakdari, H., Ebtehaj, I., & Michelson, D. G. (2018a). A combined adaptive neuro-fuzzy inference system–firefly algorithm model for predicting the roller length of a hydraulic jump on a rough channel bed. *Neural Computing and Applications*, 29, 249-258. <https://doi.org/10.1007/s00521-016-2560-9>.
- Azimi, H., Bonakdari, H., Ebtehaj, I., Gharabaghi, B., & Khoshbin, F. (2018b). Evolutionary design of generalized group method of data handling-type neural network for estimating the hydraulic jump roller length. *Acta Mechanica*, 229, 1197-1214. <https://doi.org/10.1007/s00707-017-2043-9>.
- Baylar, A., Emiroglu, M. E., & Bagatur, T. (2006). An experimental investigation of aeration performance in stepped spillways. *Water and Environment Journal*, 20(1), 35-42. <https://doi.org/10.1111/j.1747-6593.2005.00009.x>
- Benmalek, A., Hafnaoui, M. A., Madi, M., & Bensaid, M. (2023). Energy dissipation of torrential flows in different basin shapes. *Journal Algérien des Régions Arides*, 16(1), 92-100. <https://asjp.cerist.dz/en/article/229471>
- Bremen, R., & Hager, W. H. (1993). T-jump in abruptly expanding channel. *Journal of Hydraulic research*, 31(1), 61-78. <https://doi.org/10.1080/00221689309498860>.
- Carollo, F. G., Ferro, V., & Pampaloni, V. (2012). New expression of the hydraulic jump roller length. *Journal of Hydraulic Engineering*, 138(11), 995-999. [https://doi.org/10.1061/\(ASCE\)HY.1943-7900.0000634](https://doi.org/10.1061/(ASCE)HY.1943-7900.0000634)
- Chanson, H., & Brattberg, T. (2000). Experimental study of the air–water shear flow in a hydraulic jump. *International Journal of Multiphase Flow*, 26(4), 583-607. [https://doi.org/10.1016/S0301-9322\(99\)00016-6](https://doi.org/10.1016/S0301-9322(99)00016-6).
- Chen, J. Y., Liao, Y. Y., & Liu, S. I. (2013). Energy dissipation of hydraulic jump in gradually expanding channel after free overfall. *Journal of the Chinese Institute of Engineers*, 36(4), 452-457. <https://doi.org/10.1080/02533839.2012.732263>.
- Daneshfaraz, R., Aminvash, E., Esmaeli, R., Sadeghfam, S., & Abraham, J. (2020a). Experimental and numerical investigation for energy dissipation of supercritical flow in sudden contractions. *Journal of Groundwater Science and Engineering*, 8(4), 396-406. <https://doi.org/10.19637/j.cnki.2305-7068.2020.04.009>
- Daneshfaraz, R., Aminvash, E., Mirzaee, R., & Abraham, J. (2021a). Predicting the energy dissipation of a rough sudden expansion rectangular stilling basins using the SVM algorithm. *Journal of Applied Research in Water and Wastewater*, 8(2), 98-106. <https://doi.org/10.22126/arww.2021.5886.1195>
- Daneshfaraz, R., Majedi Asl, M., & Mirzaeereza, R. (2019). Experimental study of expanding effect and sand-roughened bed on hydraulic jump characteristics. *Iranian Journal of Soil and Water Research*, 50(4), 885-896. <https://doi.org/10.22059/IJSWR.2018.261923.667968>
- Daneshfaraz, R., MajediAsl, M., Mirzaee, R., & Ghaderi, A. (2020b). The S-jump’s characteristics in the rough sudden expanding stilling basin. *AUT Journal of Civil Engineering*, 4(3), 349-356. <https://doi.org/10.22060/ajce.2019.16427.5586>.
- Daneshfaraz, R., MajediAsl, M., Mirzaee, R., & Tayfur, G. (2021b). Hydraulic jump in a rough sudden symmetric expansion channel. *AUT Journal of Civil Engineering*, 5(2), 245-256. <https://doi.org/10.22060/AJCE.2020.18227.5667>.
- Daneshfaraz, R., Sadeghfam, S., Aminvash, E., & Abraham, J. P. (2022). Experimental investigation of multiple supercritical flow states and the effect of hysteresis on the relative residual energy in sudden and gradual contractions. *Iranian Journal of Science and Technology, Transactions of Civil Engineering*, 46(5), 3843-3858. <https://doi.org/10.1007/s40996-022-00818-9>
- Daneshfaraz, R., Sadeghi, H., Joudi, A. R., & Abraham, J. (2017). Experimental investigation of hydraulic jump characteristics in contractions and expansions. *Sigma Journal of Engineering and Natural Sciences*, 35(1), 87-98. <https://sigma.yildiz.edu.tr/article/475>
- Daneshfaraz, R., Santos, C. A. G., Norouzi, R., Kashani, M. H., AmirRahmani, M., & Band, S. S. (2023). Prediction of drop relative energy dissipation based on Harris Hawks Optimization algorithm. *Iranian Journal of Science and Technology, Transactions of Civil Engineering*, 47(2), 1197-1210. <https://doi.org/10.1007/s40996-022-00987-7>
- Ead, S. A., & Rajaratnam, N. (2002). Hydraulic jumps on corrugated beds. *Journal of Hydraulic Engineering*, 128(7), 656-663. [https://doi.org/10.1061/\(ASCE\)0733-9429\(2002\)128:7\(656\)](https://doi.org/10.1061/(ASCE)0733-9429(2002)128:7(656))
- Ebrahimiyan, S., Hajikandi, H., Shafai Bejestan, M., Jamali, S., & Asadi, E. (2021). Numerical study on the effect of sediment concentration on jump characteristics in trapezoidal channels. *Iranian*



- Journal of Science and Technology, Transactions of Civil Engineering*, 45, 1059-1075. <https://doi.org/10.1007/s40996-020-00510-w>.
- Elaswad, S., Saleh, O. K., & Elnikhili, E. (2022). Performance of Screen in a Sudden Expanding Stilling Basin under the Effect of the Submerged Hydraulic Jump. *The Open Civil Engineering Journal*, 16, 1-14. <https://doi.org/10.2174/18741495-v16-e2201060>.
- Gul, E., Dursun, O. F., & Mohammadian, A. (2021). Experimental study and modeling of hydraulic jump for a suddenly expanding stilling basin using different hybrid algorithms. *Water Supply*, 21(7), 3752-3771. <https://doi.org/10.2166/ws.2021.139>.
- Gupta, S. K., & Dwivedi, V. K. (2023). Prediction of depth ratio, jump length and energy loss in sloped channel hydraulic jump for environmental sustainability. *Evergreen*, 10 (2), 942-952. <https://doi.org/10.5109/6792889>
- Gupta, S. K., & Dwivedi, V. K. (2024a). Effect of surface roughness and channel slope on hydraulic jump characteristics: an experimental approach towards sustainable environment. *Iranian Journal of Science and Technology, Transactions of Civil Engineering*, 48(3), 1695-1713. <https://doi.org/10.1007/s40996-023-01246-z>.
- Gupta, S. K., & Dwivedi, V. K. (2024b). Experimental investigation of hydraulic jump characteristics in sloping rough surfaces for sustainable development. *Engineering Research Express*, 6(2), 025103. <https://doi.org/10.1088/2631-8695/ad3acf>
- Gupta, S. K., Mehta, R. C., & Dwivedi, V. K. (2013). Modeling of relative length and relative energy loss of free hydraulic jump in horizontal prismatic channel. *Procedia Engineering*, 51, 529-537. <https://doi.org/10.1016/j.proeng.2013.01.075>
- Hafnaoui, M. A., & Debabeche, M. (2023). Displacement of a hydraulic jump in a rectangular channel: experimental study. *Iranian Journal of Science and Technology, Transactions of Civil Engineering*, 47(2), 1181-1188. <https://doi.org/10.1007/s40996-022-00974-y>.
- Hager, W. H., & Bremen, R. (1989). Classical hydraulic jump: sequent depths. *Journal of Hydraulic Research*, 27(5), 565-585. <https://doi.org/10.1080/00221688909499111>
- Hamidinejad, A. E., Heidarpour, M., & Ghadampour, Z. (2023). Hydraulic jump control using stilling basin with abruptly expanding and negative step. *Iranian Journal of Science and Technology, Transactions of Civil Engineering*, 47(6), 3885-3894. <https://doi.org/10.1007/s40996-023-01143-5>.
- Hasanabadi, H. N., Kavianpour, M. R., Khosrojerdi, A., & Babazadeh, H. (2023). Experimental study of natural bed roughness effect on hydraulic condition and energy dissipation over chutes. *Iranian Journal of Science and Technology, Transactions of Civil Engineering*, 47(3), 1709-1721. <https://doi.org/10.1007/s40996-023-01060-7>
- Hassanpour, N., Hosseinzadeh Dalir, A., Farsadzadeh, D., & Gualtieri, C. (2017). An experimental study of hydraulic jump in a gradually expanding rectangular stilling basin with roughened bed. *Water*, 9(12), 945. <https://doi.org/10.3390/w9120945>
- Herbrand, K. (1973). The spatial hydraulic jump. *Journal of Hydraulic Research*, 11 (3), 205-217. <https://doi.org/10.1080/00221687309499774>
- Jan, C. D., & Chang, C. J. (2009). Hydraulic jumps in an inclined rectangular chute contraction. *Journal of Hydraulic Engineering*, 135(11), 949-958. [https://doi.org/10.1061/\(ASCE\)HY.1943-7900.0000100](https://doi.org/10.1061/(ASCE)HY.1943-7900.0000100).
- Kim, Y., Choi, G., Park, H., & Byeon, S. (2015). Hydraulic jump and energy dissipation with sluice gate. *Water*, 7(9), 5115-5133. <https://doi.org/10.3390/w7095115>
- Kramer, M., & Valero, D. (2020). Turbulence and self-similarity in highly aerated shear flows: The stable hydraulic jump. *International Journal of Multiphase Flow*, 129, 103316. <https://doi.org/10.1016/j.ijmultiphaseflow.2020.103316>
- Kucukali, S. E. R. H. A. T., & Cokgor, S. (2009). Energy concept for predicting hydraulic jump aeration efficiency. *Journal of Environmental Engineering*, 135(2), 105-107. [https://doi.org/10.1061/\(ASCE\)0733-9372\(2009\)135:2\(105\)](https://doi.org/10.1061/(ASCE)0733-9372(2009)135:2(105)).
- Maryami, E., Mohammadpour, R., Beirami, M. K., & Haghghi, A. T. (2021). Prediction of hydraulic jump characteristics in a closed conduit using numerical and analytical methods. *Flow Measurement and Instrumentation*, 82, 102071. <https://doi.org/10.1016/j.flowmeasinst.2021.102071>
- Matin, M. A., Hasan, M., & Islam, M. A. (2008). Experiment on hydraulic jump in sudden expansion in a sloping rectangular channel. *Journal of Civil Engineering (IEB)*, 36(2), 65-77. [https://www.jce-ieb.org/doc\\_file/3602001.pdf](https://www.jce-ieb.org/doc_file/3602001.pdf)
- McCorquodale, J. A., & Mohamed, M. S. (1994). Hydraulic jumps on adverse slopes. *Journal of Hydraulic Research*, 32(1), 119-130. <https://doi.org/10.1080/00221689409498793>
- Mnassri, S., & Triki, A. (2023). An investigation of induced free-surface wave oscillations in prismatic open-channel. *ISH Journal of Hydraulic Engineering*, 29(5), 701-706. <https://doi.org/10.1080/09715010.2022.2138587>.
- Mohammadzadeh-Habili, J., Heidarpour, M., & Samiee, S. (2018). Study of energy dissipation and downstream flow regime of labyrinth weirs. *Iranian Journal of Science and Technology, Transactions of Civil Engineering*, 42, 111-119. <https://doi.org/10.1007/s40996-017-0088-6>
- Murzyn, F., & Chanson, H. (2008). Experimental

- assessment of scale effects affecting two-phase flow properties in hydraulic jumps. *Experiments in Fluids*, 45, 513-521. <https://doi.org/10.1007/s00348-008-0494-4>
- Omid, M. H., Esmaeeli Varaki, M., Narayanan, R., Zhang, J. M., Xu, W. L., Lin, P. Z., & Wang, W. (2009). Gradually expanding hydraulic jump in a trapezoidal channel. *Journal of Hydraulic Research*, 47(3), 396-398. <https://doi.org/10.1080/00221686.2007.9521786>
- Parsaie, A., Haghiabi, A. H., Saneie, M., & Torabi, H. (2018). Prediction of energy dissipation of flow over stepped spillways using data-driven models. *Iranian Journal of Science and Technology, Transactions of Civil Engineering*, 42, 39-53. <https://doi.org/10.1007/s40996-017-0060-5>.
- Peterka, A. J. (1958). *Hydraulic design of stilling basins and energy dissipaters engineering monograph No. 25*. US Bureau of Reclamation, Denver Colorado.
- Pourabdollah, N., Heidarpour, M., Abedi Koupai, J., & Mohamadzadeh-Habili, J. (2022). Hydraulic jump control using stilling basin with adverse slope and positive step. *ISH Journal of Hydraulic Engineering*, 28(1), 10-17. <https://doi.org/10.1080/09715010.2020.1812008>
- Rajaratnam, N., & Subramanya, K. (1968). Hydraulic jumps below abrupt symmetrical expansions. *Journal of the Hydraulics Division*, 94(2), 481-504. <https://doi.org/10.1061/JYCEAJ.0001780>.
- Roushangar, K., & Homayounfar, F. (2019). Prediction characteristics of free and submerged hydraulic jumps on horizontal and sloping beds using SVM method. *KSCE Journal of Civil Engineering*, 23(11), 4696-4709. <https://doi.org/10.1007/s12205-019-1070-6>.
- Sharoonizadeh, S., Ahadiyan, J., Fathi Moghadam, M., Sajjadi, M., & Di Bacco, M. (2022). Experimental investigation on the characteristics of hydraulic jump in expanding channels with a water jet injection system. *Journal of Hydraulic Structures*, 7(4), 58-75. <https://doi.org/10.22055/JHS.2022.40233.1203>
- Torkamanzad, N., Hosseinzadeh Dalir, A., Salmasi, F., & Abbaspour, A. (2019). Hydraulic jump below abrupt asymmetric expanding stilling basin on rough bed. *Water*, 11(9), 1756. <https://doi.org/10.3390/w11091756>.
- Varaki, M. E., Kasi, A., Farhoudi, J., & Sen, D. (2014). Hydraulic jump in a diverging channel with an adverse slope. *Iranian Journal of Science and Technology, Transactions of Civil Engineering*, 38(C1), 111. <https://doi.org/10.22099/IJSTC.2014.1848>.
- Wang, W., Baayoun, A., & Khayat, R. E. (2023). A coherent composite approach for the continuous circular hydraulic jump and vortex structure. *Journal of Fluid Mechanics*, 966, A15. <https://doi.org/10.1017/jfm.2023.374>
- Welahettige, P., Lie, B., & Vaagsaether, K. (2017). Flow regime changes at hydraulic jumps in an open Venturi channel for Newtonian fluid. *The Journal of Computational Multiphase Flows*, 9(4), 169-179. <https://doi.org/10.1177/1757482X17722890>
- Zhang, J., Zhang, Q., Wang, T., Li, S., Diao, Y., Cheng, M., & Baruch, J. (2017). Experimental study on the effect of an expanding conjunction between a spilling basin and the downstream channel on the height after jump. *Arabian Journal for Science and Engineering*, 42, 4069-4078. <https://doi.org/10.1007/s13369-017-2568-1>.